

## Status of OpenLoops and Simulation of $H \rightarrow WW$ Backgrounds

---

**Fabio Cascioli,<sup>a</sup> Stefan Höche,<sup>b</sup> Frank Krauss,<sup>c</sup> Philipp Maierhöfer\*,<sup>a</sup>  
Stefano Pozzorini,<sup>a</sup> and Frank Siegert<sup>d</sup>**

<sup>a</sup>*Institut für Theoretische Physik, Universität Zürich, 8057 Zürich, Switzerland*

<sup>b</sup>*SLAC National Accelerator Laboratory, Menlo Park, CA 94025, USA*

<sup>c</sup>*Institute for Particle Physics Phenomenology, Durham University, Durham DH1 3LE, UK*

<sup>d</sup>*Institut für Kern- und Teilchenphysik, TU Dresden, D-01062 Dresden, Germany*

*E-mail:* [cascioli@physik.uzh.ch](mailto:cascioli@physik.uzh.ch), [shoeche@slac.stanford.edu](mailto:shoeche@slac.stanford.edu),  
[frank.krauss@durham.ac.uk](mailto:frank.krauss@durham.ac.uk), [philipp@physik.uzh.ch](mailto:philipp@physik.uzh.ch),  
[pozzorin@physik.uzh.ch](mailto:pozzorin@physik.uzh.ch), [frank.siegert@cern.ch](mailto:frank.siegert@cern.ch)

We report on the OPENLOOPS generator for one-loop matrix elements, which combines a numerical recursion to construct the numerator of one-loop Feynman diagrams as functions of the loop momentum with tensor integral reduction. We interfaced OPENLOOPS to the SHERPA Monte Carlo event generator in order to fully automate the simulation of next-to-leading order scattering processes. Within the SHERPA+OPENLOOPS framework we study  $H \rightarrow WW^*$  background simulations in exclusive jet bins, achieving next-to-leading order plus parton shower accuracy in the 0- and 1-jet bins.

*11th International Symposium on Radiative Corrections (Applications of Quantum Field Theory to Phenomenology)*

*22-27 September 2013*

*Lumley Castle Hotel, Durham, UK*

---

\*Speaker.

## 1. Introduction

The increasing demand for simulations of next-to-leading order (NLO) multi-particle scattering processes, which are required for the analysis of the data taken at the Large Hadron Collider, stimulated the improvement and development of tools to perform such calculations. For example, the approach based on tensor integral reduction and algebraic methods was pushed to processes which involve up to 6 external particles [1, 2]. While this method can lead to efficient code its applicability is limited by expensive algebraic simplifications and the size of the process specific code. On the other hand the application of on-shell reduction techniques e. g. in combination with tree-level recursions lead to a high degree of automation of one-loop generators [3–8].

The open loops algorithm [9] exhibits a new way to calculate loop amplitudes using a tree-like recursion for loop momentum polynomials [10] and tensor integrals. The algorithm can be fully automated and achieves high efficiency and numerical stability. A generator based on a similar approach with a Dyson-Schwinger recursion and tensor integrals was presented in [11].

We interfaced our OPENLOOPS implementation [9] to the SHERPA Monte Carlo event generator [12] which provides us with Monte Carlo integration, MC@NLO matching [13–15] to the SHERPA parton shower and MEPS@NLO multi-jet merging [16, 17]. Within this framework we calculated QCD corrections to four lepton production as a background to  $H \rightarrow WW^* \rightarrow \ell\nu\ell\nu$  [18]. After the discovery of the Higgs boson [19, 20] this channel continues to play an important role in the investigation of its properties. To render the signal visible it is necessary to apply jet vetoes and perform the analysis in exclusive jet bins, in particular to suppress the background due to  $t\bar{t}$  production. The MEPS@NLO method allows us to retain NLO accuracy in the individual jet bins and resum potentially large logarithms.

The production of two W-bosons including leptonic decays was studied extensively in the literature [21–26] and also matched to parton showers with the MC@NLO [13] and with the POWHEG method [27, 28]. W-pair production in association with a jet [29–31] has been studied as well, however previously to our simulation not matched to a parton shower. Gluon induced channels, a finite and gauge invariant subset of NNLO corrections, and their potentially sizeable impact, were studied as well [32–35].

In section 2 we briefly discuss the concepts of the open loops algorithm and in section 3 we introduce the SHERPA+OPENLOOPS framework. Selected results for the four lepton production are shown in section 4.

## 2. The OPENLOOPS matrix element generator

The generation of matrix elements with OPENLOOPS is divided in two phases. In the first step the process generator which is implemented in MATHEMATICA generates FORTRAN code which is then compiled to a process specific library. In the second step this library is used to calculate matrix elements for given parameters and phase space points. The process generator starts from a Feynman-diagrammatic representation of tree and loop amplitudes, which is obtained with the help of FEYNARTS [36], allowing for the factorisation of colour factors from the Lorentz structure of the diagrams. This way the colour reduction can be done once per process, resulting in negligible CPU cost for the colour summation [37].

Colour stripped tree diagrams are calculated by recursively connecting “sub-trees” starting from external wave functions. A sub-tree which is obtained from a tree diagram by cutting a line is represented as four complex numbers for its vector resp. spinor wave function. Colour stripped  $n$ -point loop diagrams are regarded as ordered sets of sub-trees  $\mathcal{I}_n = \{i_1, \dots, i_n\}$ , connected by loop propagators,

$$\delta\mathcal{A}^{(d)} = \int \frac{d^D q \mathcal{N}(\mathcal{I}_n; q)}{D_0 D_1 \dots D_{n-1}} = \text{Diagram} \quad (2.1)$$

The denominators  $D_i = (q + p_i)^2 - m_i^2 + i\epsilon$  depend on the loop momentum  $q$ , external momenta  $p_i$ , and internal masses  $m_i$ . All other contributions from loop propagators, vertices, and external sub-trees are summarised in the numerator, which is a polynomial of degree  $R \leq n$  in the loop momentum,

$$\mathcal{N}(\mathcal{I}_n; q) = \sum_{r=0}^R \mathcal{N}_{\mu_1 \dots \mu_r}(\mathcal{I}_n) q^{\mu_1} \dots q^{\mu_r}. \quad (2.2)$$

Momentum-shift ambiguities are eliminated by setting  $p_0 = 0$ , singling out the  $D_0$  propagator at which the loop is cut open. The loop momentum  $q$  flowing through this propagator is marked by an arrow in (2.1), defining the direction in which vertices and propagators are connected to numerically construct the tensors  $\mathcal{N}_{\mu_1 \dots \mu_r}(\mathcal{I}_n)$ . A new open Lorentz index  $\mu_i$  is added for each loop momentum which is encountered in the Feynman rules.

Inserting eq. (2.2) into eq. (2.1) results in the tensor integral representation of loop diagrams,

$$\delta\mathcal{A}^{(d)} = \sum_{r=0}^R \mathcal{N}_{\mu_1 \dots \mu_r}(\mathcal{I}_n) T_n^{\mu_1 \dots \mu_r} \quad \text{with} \quad T_n^{\mu_1 \dots \mu_r} = \int \frac{d^D q q^{\mu_1} \dots q^{\mu_r}}{D_0 D_1 \dots D_{n-1}}. \quad (2.3)$$

In order to evaluate the loop diagram, besides the coefficients  $\mathcal{N}_{\mu_1 \dots \mu_r}(\mathcal{I}_n)$  which are calculated by the open loops algorithm, one needs to evaluate the tensor integrals  $T_n^{\mu_1 \dots \mu_r}$ . For this purpose we use the COLLIER library which implements the Denner-Dittmaier tensor reduction procedure [38, 39] and the scalar integrals of ref. [40]. COLLIER cures numerical instabilities which arise due to vanishing Gram determinants and other kinematic quantities by applying expansions in these quantities, thus allowing for the numerically stable evaluation of tensor integrals in double precision. Alternatively, the OPP method [41] avoids tensor integrals through a direct connection between the numerator  $\mathcal{N}(\mathcal{I}_n; q)$  and the scalar-integral representation of the amplitude. The coefficients of the scalar integrals are determined by multiple evaluations of  $\mathcal{N}(\mathcal{I}_n; q)$  for loop momenta  $q$  which satisfy multiple-cut conditions of the form  $D_i = D_j = \dots = 0$ . With the knowledge of the the coefficients  $\mathcal{N}_{\mu_1 \dots \mu_r}(\mathcal{I}_n)$ , eq. (2.2) allows for very fast evaluations of the numerator function for given values of the loop momentum.

Rational terms of type  $R_2$  are reconstructed by counterterm-like Feynman rules [42]. In order to asses the performance and the numerical stability we considered the  $2 \rightarrow 2, 3, 4$  reactions  $u\bar{u} \rightarrow$

W/Z	$\gamma$	jets	HQ pairs	single-top	Higgs
$V + 3j$	$\gamma + 3j$	$3(4)j$	$t\bar{t} + 1j$	$tb + 1j$	$(H + 2j)$
$VV + 1(2)j$	$\gamma\gamma + 1(2)j$		$t\bar{t}V + 0(1)j$	$t + 1(2)j$	$VH + 1j$
$gg \rightarrow VV + 1j$	$V\gamma + 1(2)j$		$b\bar{b}V + 0(1)j$	$tW + 0(1)j$	$t\bar{t}H$
$VVV + 0(1)j$					$qq \rightarrow Hqq + 0(1)j$

**Table 1:** Processes which are available to the ATLAS and CMS Monte Carlo working groups. Vector boson production ( $V = Z/W^\pm$ ) includes leptonic decays except for  $VVV$ . Lower jet multiplicities are implicitly understood. Brackets denote that the process will be available with the next update.

$W^+W^- + ng$ ,  $u\bar{d} \rightarrow W^+g + ng$ ,  $u\bar{u} \rightarrow t\bar{t} + ng$ , and  $gg \rightarrow t\bar{t} + ng$ , with  $n = 0, 1, 2$  gluons [9]. For the most complicated  $2 \rightarrow 4$  processes the runtime per phase space point is below 1 second on an i5-750 CPU (single core) and the size of a compiled process library is of the order of at most 1 MB. The average number of correct digits ranges from 11 to 15 for the 12 processes and the probability to encounter numerical precision below  $10^{-5}$  and  $10^{-3}$  is less than 2 and 0.1 per mil, respectively.

Recently, the OPENLOOPS program was applied in first phenomenological studies. Besides the four lepton production which is discussed here, it was used in the simulation of  $t\bar{t}b\bar{b}$  production with massive b quarks, matched to the SHERPA parton shower [43],  $W^+W^-b\bar{b}$  with massive b quarks [44], describing off-shell effects in  $t\bar{t}$  production in the full b quark phase space, and for the real-virtual corrections in NNLO  $Z\gamma$  production [45], i. e.  $Z\gamma + j$  including soft jet emission which is particularly challenging with respect to the numerical stability.

### 3. NLO automation with SHERPA+OPENLOOPS

To fully automate NLO simulations, the matrix element generator must be interfaced to a Monte Carlo event generator. We chose the SHERPA event generator which, in particular, provides us with infra-red subtraction, real emission, phase space integration, MC@NLO matching to its parton shower, and MEPS@NLO merging of different jet multiplicities, providing NLO plus parton shower accuracy in the individual jet bins. Especially for the description of exclusive observables the resummation of large logarithms as provided by a parton shower is imperative. The matrix element generation is steered by standard SHERPA runcards.

The SHERPA+OPENLOOPS framework is available to the Monte Carlo working groups of the ATLAS and CMS collaborations, including the set of processes shown in table 1. All provided processes were thoroughly validated against an independent in-house matrix element generator.

### 4. Irreducible background to $H \rightarrow WW$

We used SHERPA+OPENLOOPS<sup>1</sup> for the simulation of  $\mu^+ \nu_\mu e^- \bar{\nu}_e (+j)$  production (in the following referred to as 4 leptons or  $4\ell(+j)$ ) as irreducible background to  $H \rightarrow WW^*$  at a centre-of-mass energy of 8 TeV, including off-shell and non-resonant contributions and all respective interferences [18]. To assess the effects of the parton shower and the merging we calculated the processes in three different approximations, fixed order NLO, MC@NLO, and MEPS@NLO.

<sup>1</sup>Results were obtained with a pre-release version of SHERPA 2.0 corresponding to SVN revision 21825.

0-jet bin	NLO $4\ell$	MC@NLO $4\ell$	MEPS@NLO $4\ell+0, 1j$	MEPS@LOOP <sup>2</sup> $4\ell+0, 1j$
$\sigma_S$ [fb]	34.28(9) <sup>+2.1%</sup> <sub>-1.6%</sub>	32.52(8) <sup>+2.1%</sup> <sub>-0.8%</sub> <sup>+1.2%</sup> <sub>-0.7%</sub>	33.81(12) <sup>+1.4%</sup> <sub>-2.2%</sub> <sup>+2.0%</sup> <sub>-0.4%</sub>	1.98(2) <sup>+23%</sup> <sub>-16.5%</sub> <sup>+27%</sup> <sub>-20%</sub>
$\sigma_C$ [fb]	55.76(9) <sup>+2.0%</sup> <sub>-1.7%</sub>	52.28(9) <sup>+1.4%</sup> <sub>-0.7%</sub> <sup>+1.4%</sup> <sub>-1.1%</sub>	54.18(15) <sup>+1.4%</sup> <sub>-1.9%</sub> <sup>+2.5%</sup> <sub>-0.4%</sub>	2.41(2) <sup>+22%</sup> <sub>-17%</sub> <sup>+27%</sup> <sub>-18%</sub>
1-jet bin	NLO $4\ell + j$	MC@NLO $4\ell + j$	MEPS@NLO $4\ell+0, 1j$	MEPS@LOOP <sup>2</sup> $4\ell+0, 1j$
$\sigma_S$ [fb]	8.99(4) <sup>+4.9%</sup> <sub>-9.5%</sub>	8.02(4) <sup>+8.5%</sup> <sub>-6.4%</sub> <sup>+0%</sup> <sub>-3.1%</sub>	9.37(9) <sup>+2.6%</sup> <sub>-2.7%</sub> <sup>+2.5%</sup> <sub>-0.0%</sub>	0.46(1) <sup>+40%</sup> <sub>-18%</sub> <sup>+2.2%</sup> <sub>-6.3%</sub>
$\sigma_C$ [fb]	26.50(8) <sup>+6.4%</sup> <sub>-12.5%</sub>	24.58(8) <sup>+6.1%</sup> <sub>-6.5%</sub> <sup>+1.2%</sup> <sub>-3.0%</sub>	28.32(13) <sup>+3.1%</sup> <sub>-4.7%</sub> <sup>+4.1%</sup> <sub>-0.0%</sub>	0.79(1) <sup>+33%</sup> <sub>-20%</sub> <sup>+15%</sup> <sub>-7%</sub>

**Table 2:** Exclusive 0- and 1-jet bin  $\mu^+ \nu_\mu e^- \bar{\nu}_e + \text{jets}$  cross sections in the signal (S) and control (C) regions of the ATLAS analysis at 8 TeV. Fixed-order NLO results are compared to MC@NLO and MEPS@NLO predictions. The squared quark-loop contributions (MEPS@LOOP<sup>2</sup>) are shown separately. Scale uncertainties are shown as  $\sigma \pm \delta_{\text{QCD}} \pm \delta_{\text{res}}$ , where  $\delta_{\text{QCD}}$  and  $\delta_{\text{res}}$  correspond to variations of the QCD ( $\mu_R, \mu_F$ ) and resummation ( $\mu_Q$ ) scales, respectively. Statistical errors are given in parenthesis.

The vector bosons are treated in the complex mass scheme, and the electroweak mixing angle is obtained from the complex W- and Z-boson masses [46]. The electromagnetic fine-structure constant is derived from the Fermi constant in the  $G_\mu$ -scheme. As parton distribution functions we chose five-flavour CT10 NLO [47] with the respective running strong coupling  $\alpha_S$ . The renormalisation ( $\mu_R$ ), factorisation ( $\mu_F$ ) and resummation ( $\mu_Q$ ) scales are chosen as the average transverse energy of the W bosons, and QCD scale uncertainties are estimated by factor 2 variations of  $\mu_R$  and  $\mu_F$ , and  $\sqrt{2}$  variations of  $\mu_Q$ . In the parton shower and for the jet emission in the  $4\ell + j$  matrix elements for the MEPS@NLO simulation the scale choice is based on the CKKW technique which adapts the  $\alpha_S$  scale to the transverse momentum of the jet. The merging scale  $Q_{\text{cut}}$  is set to 20 GeV. The values for the input parameters and a detailed description of the setup can be found in [18].

To avoid any overlap with  $t\bar{t}$  production, only partonic channels without external b quarks are considered. This requires a prescription to separate  $W^+W^- + j$  from top pair and single top production which treats infrared singularities and large logarithms arising from  $g \rightarrow b\bar{b}$  splittings in a well defined way [18]. Such a prescription is not unique and reflects in an ambiguity of the order of 1% which disappears when  $W^+W^- + j$  and  $W^+W^-b\bar{b}$  are consistently merged.

We also studied squared quark-loop contributions, which are formally of next-to-next-to-leading order but can give sizable contributions to the cross section due to the large gluon flux in high energy proton collisions. In the 1-jet contribution, for consistent merging also quark-loop diagrams with external quarks must be included in order to account for  $g \rightarrow q\bar{q}$  splittings in the parton shower. This leads to  $\mathcal{O}(\pm 50\%)$  shape distortions in the  $p_T$  distribution of the squared quark-loop contribution.

In the experimental analyses a data driven approach is used, in which Monte Carlo simulations are normalised to data in a signal free phase space region (control region) and extrapolated to the signal region. The extrapolation uncertainties cannot be reliably assessed by scale variations. The squared loop contributions introduce genuine NNLO kinematic effects, which we assume to be of similar size as the unknown NNLO effects. For the ATLAS setup we find an extrapolation uncertainty of 1.3% in the 0-jet bin and 2.1% in the 1-jet bin.

Table 2 shows the cross sections for the three simulations with different perturbative accuracy as well as the squared quark-loop cross sections in the signal and control regions of the ATLAS

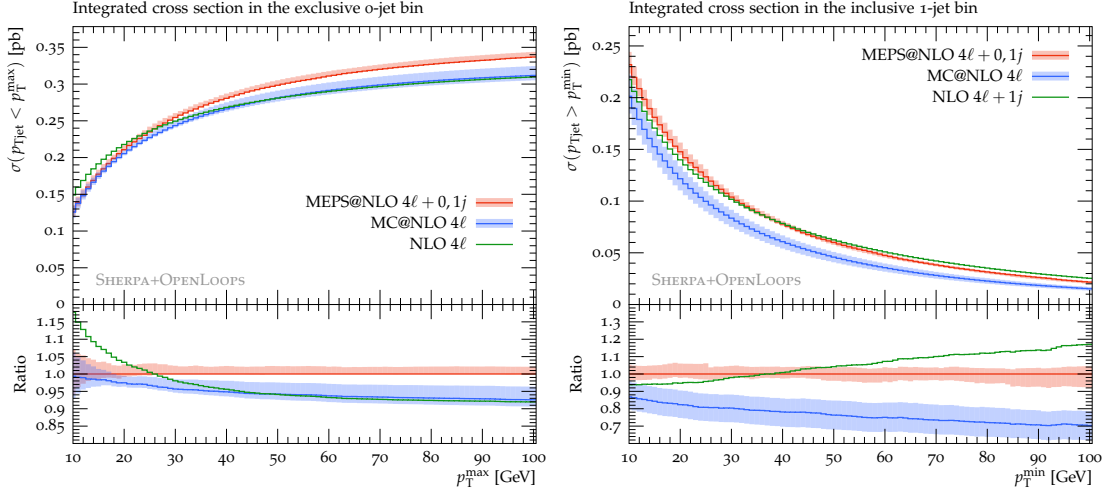


**Figure 1:** Integrated cross sections in the exclusive 0-jet bin (left) and in the inclusive 1-jet bin (right) as a function of the jet veto scale  $p_T^{\max}$ , respectively  $p_T^{\min}$ . NLO results (green) are compared to MC@NLO 4 $\ell$ (blue) and MEPS@NLO 4 $\ell$ +0, 1j(red) simulations. Uncertainty bands correspond to QCD-scale variations quadratically combined with the resummation-scale variations.

analysis. Corresponding results for the CMS analysis can be found in [18].

Figure 4 illustrates the matching and merging effects in the presence of a jet veto. The integrated cross sections in the exclusive 0-jet bin and in the inclusive 1-jet bin are plotted against the upper transverse momentum bound  $p_T^{\max}$ , resp. lower bound  $p_T^{\min}$ . In the 0-jet bin the simulations differ by  $\mathcal{O}(5\%)$  for typical values of  $p_T^{\max} \sim 25 - 30$  GeV and Sudakov effects are moderate. In the 1-jet bin the MC@NLO simulation differs by 20 – 30% from the MEPS@NLO simulation, reflecting the leading-order only accuracy of MC@NLO in the 1-jet bin. Scale variation uncertainties of the MEPS@NLO simulation amount to a few percent. In the full analysis [18] we study various other observables which are relevant for the experimental analysis.

## 5. Conclusions

We interfaced OPENLOOPS, an automatic generator for one-loop matrix elements based on the numerical construction of loop momentum polynomials and tensor integral reduction, with the SHERPA Monte Carlo event generator.

Within the SHERPA+OPENLOOPS framework we performed detailed simulations of the production of 4 leptons with up to one jet as a background for the  $H \rightarrow WW^*$  analysis of the ATLAS and CMS experiments and studied the impact of parton shower and merging effects. The MEPS@NLO simulation provides NLO accuracy and resummation in both jet bins and exhibits scale uncertainties below 5%. This approach is particularly suited to study exclusive observables and provides more realistic error estimates. In our simulation we included the effects due to squared quark-loop contributions and used them for a reliable estimate of the uncertainties that arise from kinematic distortions introduced by unknown NNLO corrections.

SHERPA+OPENLOOPS will be published soon and is already available to the ATLAS and CMS Monte Carlo working groups including libraries for a wide range of processes.

## Acknowledgments

The research of F. Cascioli, P. Maierhöfer and S. Pozzorini was supported by the SNSF. Stefan Höche was supported by the U.S. Department of Energy under Contract No. DE-AC02-76SF00515.

## References

- [1] A. Bredenstein, A. Denner, S. Dittmaier, and S. Pozzorini, *Phys. Rev. Lett.* **103** (2009) 012002 [arXiv:0905.0110].
- [2] A. Denner, S. Dittmaier, S. Kallweit, and S. Pozzorini, *Phys. Rev. Lett.* **106** (2011) 052001 [arXiv:1012.3975].
- [3] R. K. Ellis, W. T. Giele, Z. Kunszt, and K. Melnikov, *Nucl. Phys. B* **822** (2009) 270 [arXiv:0806.3467].
- [4] C. F. Berger, Z. Bern, L. J. Dixon, F. Febres Cordero, D. Forde, H. Ita, D. A. Kosower, and D. Maitre, *Phys. Rev. D* **78** (2008) 036003 [arXiv:0803.4180].
- [5] V. Hirschi, R. Frederix, S. Frixione, M. V. Garzelli, F. Maltoni, and R. Pittau, *JHEP* **1105** (2011) 044 [arXiv:1103.0621].
- [6] G. Cullen, N. Greiner, G. Heinrich, G. Luisoni, P. Mastrolia, G. Ossola, T. Reiter, and F. Tramontano, *Eur. Phys. J. C* **72** (2012) 1889 [arXiv:1111.2034].
- [7] G. Bevilacqua, M. Czakon, M. V. Garzelli, A. van Hameren, A. Kardos, C. G. Papadopoulos, R. Pittau, and M. Worek, *Comput. Phys. Commun.* **184** (2013) 986 [arXiv:1110.1499].
- [8] S. Badger, B. Biedermann, P. Uwer, and V. Yundin, *Comput. Phys. Commun.* **184** (2013) 1981 [arXiv:1209.0100].
- [9] F. Cascioli, P. Maierhofer, and S. Pozzorini, *Phys. Rev. Lett.* **108** (2012) 111601 [arXiv:1111.5206].
- [10] A. van Hameren, *JHEP* **0907** (2009) 088 [arXiv:0905.1005].
- [11] S. Actis, A. Denner, L. Hofer, A. Scharf, and S. Uccirati, *JHEP* **1304** (2013) 037 [arXiv:1211.6316].
- [12] T. Gleisberg, S. Hoeche, F. Krauss, M. Schonherr, S. Schumann, et al., *JHEP* **0902** (2009) 007 [arXiv:0811.4622].
- [13] S. Frixione, and B. R. Webber, *JHEP* **0206** (2002) 029 [hep-ph/0204244].
- [14] S. Hoeche, F. Krauss, M. Schonherr, and F. Siegert, *JHEP* **1209** (2012) 049 [arXiv:1111.1220].
- [15] S. Hoeche, F. Krauss, M. Schonherr, and F. Siegert, *Phys. Rev. Lett.* **110** (2013) 052001 [arXiv:1201.5882].
- [16] T. Gehrmann, S. Hoeche, F. Krauss, M. Schonherr, and F. Siegert, *JHEP* **1301** (2013) 144 [arXiv:1207.5031].
- [17] S. Hoeche, F. Krauss, M. Schonherr, and F. Siegert, *JHEP* **1304** (2013) 027 [arXiv:1207.5030].
- [18] F. Cascioli, S. Hoeche, F. Krauss, P. Maierhofer, S. Pozzorini, and F. Siegert, [arXiv:1309.0500].
- [19] ATLAS Collaboration, G. Aad et al., *Phys. Lett.* **B716** (2012) 1–29 [arXiv:1207.7214].

- [20] CMS Collaboration, S. Chatrchyan et al., *Phys. Lett.* **B716** (2012) 30–61 [arXiv:1207.7235].
- [21] J. Ohnemus, *Phys. Rev.* **D44** (1991) 1403–1414.
- [22] S. Frixione, *Nucl. Phys.* **B410** (1993) 280–324.
- [23] J. Ohnemus, *Phys. Rev.* **D50** (1994) 1931–1945 [hep-ph/9403331].
- [24] L. J. Dixon, Z. Kunszt, and A. Signer, *Phys. Rev.* **D60** (1999) 114037 [hep-ph/9907305].
- [25] J. M. Campbell, and R. K. Ellis, *Phys. Rev.* **D60** (1999) 113006 [hep-ph/9905386].
- [26] J. M. Campbell, R. K. Ellis, and C. Williams, *JHEP* **1107** (2011) 018 [arXiv:1105.0020].
- [27] S. Frixione, P. Nason, and C. Oleari, *JHEP* **0711** (2007) 070 [arXiv:0709.2092].
- [28] T. Melia, P. Nason, R. Rontsch, and G. Zanderighi, *JHEP* **1111** (2011) 078 [arXiv:1107.5051].
- [29] J. M. Campbell, R. K. Ellis, and G. Zanderighi, *JHEP* **0712** (2007) 056 [arXiv:0710.1832].
- [30] S. Dittmaier, S. Kallweit, and P. Uwer, *Phys. Rev. Lett.* **100** (2008) 062003 [arXiv:0710.1577].
- [31] S. Dittmaier, S. Kallweit, and P. Uwer, *Nucl. Phys.* **B826** (2010) 18–70 [arXiv:0908.4124].
- [32] T. Binoth, M. Ciccolini, N. Kauer, and M. Kramer, *JHEP* **0503** (2005) 065, [hep-ph/0503094].
- [33] T. Binoth, M. Ciccolini, N. Kauer, and M. Kramer, *JHEP* **0612** (2006) 046, [hep-ph/0611170].
- [34] J. M. Campbell, R. K. Ellis, and C. Williams, *JHEP* **1110** (2011) 005, [arXiv:1107.5569].
- [35] T. Melia, K. Melnikov, R. Rontsch, M. Schulze, and G. Zanderighi, *JHEP* **1208** (2012) 115, [arXiv:1205.6987].
- [36] T. Hahn, *Comput. Phys. Commun.* **140** (2001) 418 [hep-ph/0012260].
- [37] A. Bredenstein, A. Denner, S. Dittmaier, and S. Pozzorini, *JHEP* **1003** (2010) 021 [arXiv:1001.4006].
- [38] A. Denner, and S. Dittmaier, *Nucl. Phys.* **B658** (2003) 175–202 [hep-ph/0212259].
- [39] A. Denner, and S. Dittmaier, *Nucl. Phys.* **B734** (2006) 62–115 [hep-ph/0509141].
- [40] A. Denner and S. Dittmaier, *Nucl. Phys.* **B844** (2011) 199–242 [arXiv:1005.2076].
- [41] G. Ossola, C. G. Papadopoulos, and R. Pittau, *Nucl. Phys.* **B763** (2007) 147–169 [hep-ph/0609007].
- [42] P. Draggiotis, M. Garzelli, C. Papadopoulos, and R. Pittau, *JHEP* **0904** (2009) 072 [arXiv:0903.0356].
- [43] F. Cascioli, P. Maierhoefer, N. Moretti, S. Pozzorini and F. Siegert, arXiv:1309.5912.
- [44] F. Cascioli, S. Kallweit, P. Maierhöfer and S. Pozzorini, [arXiv:1312.0546].
- [45] M. Grazzini, S. Kallweit, D. Rathlev and A. Torre, [arXiv:1309.7000].
- [46] A. Denner, S. Dittmaier, M. Roth, and L. Wieders, *Nucl. Phys.* **B724** (2005) 247–294 [hep-ph/0505042].
- [47] H.-L. Lai, M. Guzzi, J. Huston, Z. Li, P. M. Nadolsky, et al., *Phys. Rev.* **D82** (2010) 074024 [arXiv:1007.2241].